Freshwater plume-like condition near the north-eastern coastal Arabian Sea during early Miocene: Evidence from the stable isotope record in the growth bands of gastropods (*Turritella* sp.)

Yogaraj Banerjee[1#] and Prosenjit Ghosh[1,2]

[1]Centre for Earth Sciences, Indian Institute of Science, Bangalore 560012, India

[2]Divecha Centre for Climate Change, Indian Institute of Science, Bangalore 560012, India

#Present address: Department of Geosciences, National Taiwan University, Taipei 106, Taiwan, R.O.C

Corresponding authors: ybanerjee15@gmail.com, pghosh@iisc.ac.in

Abstract:

The Early Miocene witnessed major tectonic, palaeoceanographic and climatological reorganizations over the Asian realm. The Himalayan and Tibetan plateau upliftment influenced monsoon intensity during this age. Contemporary high-resolution tropical hydroclimate records are limited. Here, we present an early Miocene sub-annual stable isotope record from the growth bands of well-preserved *Turritella* sp. from the Kachchh basin, Western India. It showed $\delta^{13}C$ and $\delta^{18}O$ variabilities from -4.83‰ to -1.80‰ and -7.06‰ to -2.66‰ (in VPDB) respectively. Conventional oxygen isotope thermometry showed an apparent temperature seasonality from 9.3° to 28.1°C. A comparison of the present early Miocene $\delta^{18}O$ record with the modern $\delta^{18}O$ records in the carbonates from coastal-estuarine environments of the Indian Ocean confirmed a high freshwater influx into the NE Arabian Sea during the early Miocene, similar to the modern-day freshwater plume events observed in the coastal region.

Keywords: Miocene, Stable isotopes, Monsoon, Arabian sea, Freshwater, Upwelling

1. Introduction:

The Cenozoic period is unique in Earth's history, where tectonic rearrangement and freshwater availability due to the modified hydrological setup in the equatorial region induced a major climatic shift or cooling in the overall global ecosystem (Raymo and Ruddiman 1992, Yang et al., 2022). The Early Miocene is an important time window in the Cenozoic era that set the course of major oceanographic and climatological changes over the Asian landmass (Clift and Webb 2018) as a consequence of the closure of the Paratethys and resultant compartmentalization into the Mediterranean and Indian ocean (Bialik et al., 2019). Palaeoclimate reconstruction studies suggest an intensification of the Asian monsoon during the early Miocene, which coincided with the process of tectonic upliftment of the Himalaya and Tibetan plateau (HTP) complex (Clift et al., 2008; Clift 2020). Tropical records of early Miocene precipitation on a sub-annual scale are either limited or inadequate to verify the seasonal transformation of environmental conditions. However, a record of the seasonal pattern of precipitation depicting the operation of the Asian monsoon does exist for the late Miocene time from the continental interior, away from the marine settings (Dettman et al., 2001). There are multiple studies covering the early Miocene to late Miocene time period focusing on the long-term variability in the monsoon intensity over the East Asian summer monsoon region (Guo et al., 2008; Wei et al., 2006; Zhang et al., 2018). A few studies highlighted the importance of understanding the evolution of the South Asian monsoon (SAM) going back to the mid-Miocene (Gupta et al., 2015; Bialik et al., 2020). The Miocene time period is considered to be a "test bed" for exploring the future climate scenario as pCO_2 conditions approach values similar to modern day or more as projected for coming centuries (Levy et al., 2016; Steinthorsdottir et al 2021; Zammit et al., 2022). The response of SAM to high CO_2 is complicated but possible to understand through a combination of experimental observation with model-based simulation. There exists a spatial heterogeneity (Qu et al., 2022) and decoupling between SAM precipitation and circulation pattern (Sarr et al., 2022; Zhang et al., 2023) in response to the atmospheric CO_2 level. In the context of modern and future climate change scenarios, a clear understanding of the role of CO_2 on the operation of SAM at a seasonal time scale is crucial for the long-term socio-economic sustainability of the region.

Gastropods like *Turritella sp.* have been widely used as a suitable archive for deducing tropical palaeoclimate and seasonal precipitation patterns (Scholz et al., 2020 and references therein). The $\delta^{18}O$ variability recorded in their growth bands has been attributed to seasonal changes in water isotopic composition and temperature (Waite and Allomon, 2013). Due to their optimal longevity of 1.5–2 years and assuming relatively constant growth rates (Waite and Allomon, 2013), they serve as an ideal sclerochronological archive for the seasonal reconstruction of freshwater input in an estuary (Aharon 1991; Watanabe and Oba 1999; Elliot et al. 2009; Batenburg et al. 2011; Waite and Allomon, 2013).

Here in this study, we have carried out high-resolution stable isotope analysis across the growth bands of multiple well-preserved *Turritella* shells from early Miocene (Burdigalian ~20 Ma) strata of Kachchh basin, western India. We described seasonality as the amplitude of periodic fluctuation of $\delta^{18}O$ in shell growth bands, which define the extent of change in seawater temperature or salinity during summer and winter time (Harzhauser et al. 2011). The study provides the first seasonal record of hydrological conditions from the northeastern coastal Arabian Sea during the early Miocene.

2. Geological Background:

The Early Miocene sedimentary record from the Kachchh basin is divided into two stratigraphic formations, the lower Khari Nadi Formation and the upper Chhasra Formation. Khari Nadi Formation is characterized by alternate occurrences of silty shale and siltstone at the lower and middle part and a few limestone beds separated by silty shales at the upper portion (Fig. 1). The contact between these two formations is gradational. The Chhasra Formation is comprised of two members, the lower clay-rich member with discrete limestone beds of 5 to 100 cm thickness, hosting a colony of fossil gastropod of *Turritella* sp., which is intervened by silty shales and siltstone member at the top (Biswas, 1992). The ages of both these formations were assigned based on biostratigraphy. The depositional environment for sedimentation varies from tidal flat to littoral and shallow marine environment, featuring a sequence favoured for a slowly transgressive sea (Biswas and Raju 1973). The Khari Nadi Formation is assigned *Aquitanian* age based on the presence of larger foraminiferal species *Miogypsina (Miogypsina) tani* and Miogypsina *(Miogypsinoides) dehartii*. The overlying

Chhasra Formation is assigned *Burdigalian* age based on the presence of *Miogypsina (Miogypsina)globulina*. Palynofloral assemblage assessment reveals the dominance of angiospermous pollen grains over pteridophytic spores, suggesting an overall warm and humid coastal climate with tropical rainforests in a lowland coastal setting (Verma et al., 2013). This was consistent with earlier observations documenting the presence of extant species of the *Dipterocarpaceae* family supporting the existence of tropical evergreen forests in this region (Sukhla et al., 2012).

3. Materials and Methods:

Four well-preserved Early Miocene *Turritella* shells were selected from our collection for the present study. Samples were collected from a field exposure along the Kankawati River near the village of Vinjhan at N 23°50' 37.50", E 69°20' 57.20", and assigned biostratigraphy age of Burdigalian (~ 20 Ma) (Catuneanu & Dave, 2017; Halder & Bano, 2015; Kumar and Saraswati, 1997) with a probable 2 Ma age uncertainty. Visual and microscopic inspection of specimens, including XRD analysis of carbonate powder, were carried out to screen the well-preserved samples used for isotopic analysis (Supplementary S2). Shell exhibiting aragonitic mineralogy (Supplementary S3) were selected and treated with 30% H_2O_2 for 12 h at room temperature to ensure complete removal of organic matter (McConnaughey, 1989, Weizerbowski 2007) and then dried in a hot air oven at 60°C for moisture removal. Carbonate sample powder was drilled along the growth axis at 1mm intervals (Supplementary S4). We have used the "floating boat" method for the stable isotope ratios determination from the carbonates using Gasbench II following the protocol described in Rangarajan et al., (2021). The same analytical method was followed in other studies as well (Ghosh et al., 2021, Banerjee et al., 2023). In this method, a floating boat made from Pyrex glass loaded with 50ug of carbonate powder was introduced into the glass vial prefilled with 1 ml 105% phosphoric acid.

These vials loaded with samples and acid were flushed with He (99.99%) at 100 ml/min flow rate, and then samples were digested with acid for a duration of 70 minutes in a water bath, maintained at a constant temperature of 70°C. The stable isotope ratios of the CO_2 evolved during the acid digestion of carbonates were measured in the Thermo Finnigan (Bremen, Germany) MAT 253 isotope ratio mass spectrometer, coupled with a GasBench II peripheral, housed at the Stable Isotope Laboratory of Centre for Earth Sciences, Indian Institute of Science, Bangalore, India. The reproducibility of $\delta^{18}O$ and $\delta^{13}C$ were 0.04 and 0.05‰, respectively, based on replicate analysis of Carrara marble (MARJ1: $\delta^{13}C$ value 1.96% and $\delta^{18}O$ -2.01‰) reference material (Rangarajan et al., 2021; Ghosh et al., 2005).

4. Results and Discussions:

4.1 $\delta^{13}C$ variability

Previous studies documented an abundance of *Turritella* sp. in the region dominated by the process of upwelling. The inverse relationship between $\delta^{13}C$ and $\delta^{18}O$ in the growth bands signifies varying water conditions mostly encountered in upwelling processes (Geary et al., 1992; Killingley and Berger, 1979; Tao et al., 2013). Cold upwelled waters promote productivity and are characterised by isotopically heavier dissolved inorganic carbon, while deep upwelled water is less saline and carries a signature of isotopically lighter oxygen isotopic ratios (Kroopnick 1980; Tao et al., 2013). Carbon isotope ratios in the carbonate growth bands record seasonal productivity in the environment. In an open ocean system, productivity dominates over respiration, which enriches the carbon isotope ratios. Whereas in a river-dominated system, respiration is pronounced and adds isotopically lighter carbon in the inorganic reservoir. The 4 gastropod shells analysed in the study recorded periodically varying $\delta^{13}C$ values in the incremental growth chambers (Fig. 2). The shell designated as 1 showed $\delta^{13}C$ values ranging from -3.72‰ to -2.01‰ with an average value of -2.82‰. Similarly, shell

2 recorded $\delta^{13}C$ values ranging from -4.30‰ to -1.80‰ with an average value of -2.87‰. Shell 3 registered $\delta^{13}C$ values ranging from -4.83‰ to -2.20‰ with an average value of -2.93‰. The shell 4 growth bands range in $\delta^{13}C$ values from -4.39‰ to -2.66‰ with an average value of -3.32‰ (Fig 2). We have documented periodic variability of the $\delta^{13}C$ values in all the shells, marking the episodes of highest productivity (Fig. 2 and Supplementary section 5.B) and seasonal ecological stress. Previous studies (Krantz et al., 1988; Jones and Allmon 1995) have shown that mollusc shells capture signatures of isotopically lighter carbon coming from the continent (depleted $\delta^{13}C$) coupled with lighter oxygen isotopes (depleted $\delta^{18}O$) during freshwater run-off. Whereas, they register lighter carbon released during the oxidation of organic debris (depleted $\delta^{13}C$) along with heavier $\delta^{18}O$ (enriched $\delta^{18}O$) during upwelling events. In the present study, the stable isotope profiles of early Miocene *Turritella sp*. captured evidence of probable freshwater run-off as well as upwelling events similar to the previous studies (Krantz et al., 1988; Jones and Allmon 1995). The intensity of such events was not uniform, as evident from the isotopic signals of the shells studied here. Repeated occurrences of tropical cyclones and associated upwelling have been documented in the modern-day Arabian Sea region (RoyChowdhury et al., 2020; Ganguly et al., 2020). Such upwelling events can affect the isotopic signature of the coastal water of the west coast of India as well (Jacob et al.,2016). More detailed investigation can further elucidate the paleo-upwelling dynamics in this region during the early Miocene.

4.2 $\delta^{18}O_{VPDB}$ variability and freshwater influx

The factors responsible for the variation in the $\delta^{18}O$ values of the gastropod shells are both temperature and the $\delta^{18}O$ of water. Higher temperature promotes evaporative enrichment of $\delta^{18}O$, while freshwater flux due to excess rainfall or river water discharge determines the extent of lighter $\delta^{18}O$ in the carbonate growth bands. A previous study on the seasonal growth bands of bivalve shells from fluvial sediments belonging to the late Miocene age (Dettman et al., 2001) recorded $\delta^{18}O_{carb}$ variability and was related to the terrestrial $\delta^{18}O_{water}$ seasonality assuming the temperature condition inferred from the palynological assemblages retrieved from the sediments.

The $\delta^{18}O_{VPDB}$ values of growth bands in Miocene *Turritella* shells (Fig. 2) investigated in the present study oscillate with a range from -7.06‰ to -3.81‰ and an average of -5.18‰ for shell 1. Similarly, the $\delta^{18}O_{VPDB}$ value in shell 2 ranges from -6.51‰ to -3.20‰ with an average of -5.07‰. The $\delta^{18}O_{VPDB}$ value in Shell 3 ranges from -6.72‰ to -3.34‰ with an average of -4.68‰. For shell 4 the $\delta^{18}O$ values range from -5.57‰ to -2.66‰ with an average of -4.97‰ (Fig. 2B).

Individual shells captured periodic oscillatory patterns with heavier isotopic values defining the dry time, while seasonal wet period with excess freshwater discharge is characterized by lighter $\delta^{18}O$ values. The overall isotopic signatures obtained from the present study suggest a tropical coastal climate with seasonal freshwater contribution being highest during monsoon, confirming the interpretation of previous studies based on palynological assemblages (Verma et al., 2013; Rao and Verma 2014). We defined apparent seasonality as a difference between maxima and minima values of $\delta^{18}O$, representing the dry time and wet conditions.

`Apart from temperature, the hydrological condition of the basin also controls the oxygen isotope composition of shell carbonates. In case of more freshwater influx, the $\delta^{18}O$ would be lighter /negative. A higher extent of evaporation would lead to a more positive $\delta^{18}O$ value or heavier composition. We have compared early Miocene *Turritella*-based $\delta^{18}O$ record (Fig.3 and Supplementary section 6) from the Kachchh basin (eastern Arabian Sea) with the coeval $\delta^{18}O$ records from the Quilon formation (south-eastern Arabian Sea from Prasanna and Kapur 2022) and exceptionally well-preserved planktonic foraminifera from coastal Tanzania (western Arabian sea from Stewart et al., 2004). We have further compared the early Miocene $\delta^{18}O$ records with the modern-day mollusc shell-based $\delta^{18}O$ records from the western Indian coastal locations – Mandvi beach of Bhuj (Present study), MZ estuary (Ghosh et al., 2021), Cochin estuary of Southern India (Ghosh et al., 2018) and Hooghly estuary (Banerjee et al., 2018). This comparison shows the Kachchh basin, situated in the north-eastern part of the Arabian Sea was receiving more freshwater influx than the coeval basins at the south eastern (Quilon formation) coastal Arabian Sea and Tanzania representing the eastern coastal Indian Ocean. Early Miocene freshwater influx at the Kachchh basin was higher than the present-day coastal and estuarine environment of western (MZ estuary, Mandvi beach) and southern India (Cochin estuary). However, it is more similar to that of the Hooghly Estuary, located in eastern India. We consider this excess freshwater influx as a freshwater plume-like condition as documented in the modern coastal Indian Ocean (Rao et al., 2009; Joshi et al., 2021). We have estimated around 21 psu change in the apparent salinity (Supplementary section 7) due to the enhanced freshwater influx for the early Miocene Kachchh basin, comparable with the modern estimates (Seena et al., 2019).

We also noted that the $\delta^{18}O$ record from the early Miocene molluscs from Quilon formation is similar to that of the nearby modern estuarine record from the Cochin estuary. Our observation confirms a similar mode of ITCZ dynamics (Prasanna and Kapur, 2022) during the early Miocene, which controls the monsoonal precipitation (Banerjee et al., 2020). Given the similarity in the ITCZ dynamics, the more negative values in the $\delta^{18}O$ from the Kachchh basin imply contribution from an additional source of moisture during the early Miocene or involvement of moisture recycling probably due to thicker vegetation cover. Extreme events like cyclones, storms, etc., can also modify the salinity of the shelf region (Singh et al., 2000; Kumar et al., 2018). The $\delta^{18}O$ composition of mollusc shells can record the changes in the hydrological conditions related to such extreme events (Strauss et al., 2012; Leng and Lewis, 2016). Occurrences of tropical cyclones in the Paratethys region during the early Miocene have been documented by El-Shazly (2011). Some of the data points in our record may represent such extreme events. Also, the role of palaeogeography controlling the monsoonal precipitation dynamics (Tardif et al., 2023) over this region is poorly understood. A more detailed investigation involving clumped isotope thermometry will provide valuable insights into the driving mechanisms for the freshwater plume-like condition in the past.

4.3 Temperature variability:

Le´cuyer et al. (2004) have shown that the oxygen isotope composition in mollusc is a reliable recorder of the ambient water temperature. In order to estimate temperature using oxygen isotope thermometry, $\delta^{18}O_{water}$ should be either measured or precisely assumed. Miocene temperature in the present study is calculated from the measurement of shell carbonates assuming an offset value for the $\delta^{18}O_{water}$. We defined the seasonal variability of $\delta^{18}O_{water}$ from modern-day observation of seasonal water isotopic values measured in the coastal water of Kachchh and accounted for the additional offset for Miocene $\delta^{18}O_{water}$.

Previous studies (Lear et al., 2002; Stewart et al.,2004) have used a correction factor of 0.4 ‰ with respect to the modern-day open ocean value and estimated temperature with an assumption of the early Miocene mean $\delta^{18}O_{sw}$ = -0.4‰. However, such assumptions may not be exact if considered globally but vary spatially. It has been documented that the coastal region of the modern Arabian Sea is relatively less saline and recorded lighter $\delta^{18}O$ than its open ocean counterpart (Deshpande et al., 2013). The average $\delta^{18}O_{sw}$ composition of such less saline coastal water is -0.09‰. Thus, in our study, we have used a correction factor of 0.31‰ (modern coastal Arabian Sea $\delta^{18}O_{sw}$ - early Miocene mean $\delta^{18}O_{sw}$) to deduce the isotopic composition of the early Miocene coastal-estuarine water of the northeastern Arabian Sea sector. The estuarine water of river Narmada, which discharges into the Arabian Sea, varies from -5.27‰ to -2.67‰

seasonally (Kubota et al., 2015). We corrected the early Miocene $\delta^{18}O_w$ composition at the coastal-estuarine Kachchh basin, accounting for a 0.31‰ shift in the seasonal $\delta^{18}O_{sw}$, i.e., -5.58‰ to -2.98‰ with an average of -4.36‰.

We have assumed the early Miocene water composition of the Kachchh basin (at the confluence of freshwater and seawater mixing) as -4.36‰ for estimating of the seasonal temperature variability. The uncertainties in the temperature estimation are calculated using the $\delta^{18}O_{max\ and\ min}$ information ~ -2.98‰ and -5.58‰ respectively (Fig. 4A and Table 1). The temperature estimates for Shell 1 range from 12.9°C to 26.7°C with an average of 18.5°C. For Shell 2, it varies between 10.5°C to 24.2°C with an average of 18.0°C. Shell 3 grew in a temperature range of 11.4°C to 25.1°C with an average value of 16.4°C whereas for Shell 4 it varies from 8.4°C to 20.1° C with an average value of 17.6°C. We have compared the early Miocene temperature estimates with the modern-day water temperatures values from the Gulf of Kachchh and estuaries of some of the major west-flowing river systems- Narmada, Mahi River, Savarmati river estuaries (Fig. 4B). Considering the uncertainties in the early Miocene temperature estimates; the Temperature $_{max}$ is similar to that of the present day. However, we noted that the Temperature $_{min}$ in the early Miocene is cooler than that of the present day.

5. Conclusions:

The present study on isotopic investigation of the early Miocene *Turritella sp.* growth bands revealed a variability in carbon isotopic values ranging from -4.83‰ to -1.80‰ with an average of -2.99‰ ± 0.23‰ on the VPDB scale. For oxygen isotopes, it varies from -7.06‰ to -2.66‰. with an average of -4.83‰±0.21‰ on the VPDB scale. The overall isotopic signatures from the present study suggest an enhancement of freshwater discharge into the northeastern part of the coastal Arabian Sea during the early Miocene. We suggest this enhancement of freshwater input was driven by the intensification of Asian monsoon during this age as documented in other studies as well. Modern-day observations have also documented the presence of low salinity plumes in the north-eastern part of the Arabian Sea during post summer monsoon time period (Rao et al., 2009). The temperature reconstruction using conventional oxygen isotope thermometry registered a temperature variability of 9.3° to 28.1°C with an assumption of water isotopic values in the environment at seasonal time scales. The uncertainties in the temperature estimates of about 5°C can be reduced upon application of modern tools of clumped isotopes in the future.

Acknowledgements:

This project was a part of PhD thesis of Dr. Yogaraj Banerjee at the Indian Institute of Science, Bangalore. Funding was provided by the Department of Science and Technology (DST) and the Ministry of Earth Science (MoES), Government of India. We are grateful to Dr. Sunil Bajpai and Dr. Kalyan Haldar for their insights into defining the stratigraphy. We sincerely thank Dr. Ashok Sahni, Dr. Rajeev Patnaik, Dr. Ann Holbourn, Dr. Kaustubh Thirumalai for discussions.

References:

Aharon, P. (1991). Recorders of reef environment histories: stable isotopes in corals, giant clams, and calcareous algae. *Coral Reefs*, *10*, 71-90.

Banerjee, S., Ghosh, P., Banerjee, Y. and Riding, R. (2023). Oxygen isotopic composition of Paleoproterozoic seawater revealed by clumped isotope analysis of dolomite, Vempalle Formation, Cuddapah, India. *Chemical Geology*, *621*, 121356.

Banerjee, Y., Ghosh, P., Bhushan, R. and Rahul, P. (2018). Strong sea forcing and warmer winter during solar minima∼ 2765 yr BP recorded in the growth bands of Crassostrea sp. from the confluence of river Ganges, Eastern India. *Quaternary International*, *479*, 48-57.

Batenburg, S.J., Reichart, G.J., Jilbert, T., Janse, M., Wesselingh, F.P. and Renema, W. (2011). Interannual climate variability in the Miocene: High resolution trace element and stable isotope ratios in giant clams. *Palaeogeography, Palaeoclimatology, Palaeoecology*, *306*(1-2), 75-81.

Bialik, O.M., Auer, G., Ogawa, N.O., Kroon, D., Waldmann, N.D. and Ohkouchi, N. (2020). Monsoons, upwelling, and the deoxygenation of the northwestern Indian Ocean in response to middle to late Miocene global climatic shifts. *Paleoceanography and Paleoclimatology*, *35*(2), e2019PA003762.

Bialik, O.M., Frank, M., Betzler, C., Zammit, R. and Waldmann, N.D. (2019). Two-step closure of the Miocene Indian Ocean Gateway to the Mediterranean. *Scientific Reports*, *9*(1), 8842.

Biswas, S.K. (1992). Tertiary stratigraphy of Kutch. *Journal of the Palaeontological Society of India*, *37*(1-29).

Biswas, S.K. and Raju, D.S.N. (1973). The rock stratigraphic classification of the Tertiary sediments of Kutch. *Bull. ONGC, 10*(1-2), 37-46.

Bojar, A.V., Hiden, H., Fenninger, A. and Neubauer, F. (2004). Middle Miocene seasonal temperature changes in the Styrian basin, Austria, as recorded by the isotopic composition of pectinid and brachiopod shells. *Palaeogeography, Palaeoclimatology, Palaeoecology*, *203*(1-2), 95-105.

Catuneanu, O. and Dave, A. (2017). Cenozoic sequence stratigraphy of the Kachchh Basin, India. *Marine and Petroleum Geology*, *86*, 1106-1132.

Clift, P.D. (2020). Asian monsoon dynamics and sediment transport in SE Asia. *Journal of Asian Earth Sciences*, *195*, 104352.

Clift, P.D. and Webb, A.A.G. (2019). A history of the Asian monsoon and its interactions with solid Earth tectonics in Cenozoic South Asia. *Geological Society, London, Special Publications*, *483*(1), 631-652.

Clift, P.D., Hodges, K.V., Heslop, D., Hannigan, R., Van Long, H. and Calves, G. (2008). Correlation of Himalayan exhumation rates and Asian monsoon intensity. *Nature geoscience*, *1*(12), 875-880.

Deshpande, R.D., Muraleedharan, P.M., Singh, R.L., Kumar, B., Rao, M.S., Dave, M., Sivakumar, K.U. and Gupta, S.K. (2013). Spatio-temporal distributions of δ18O, δD and salinity in the Arabian Sea: Identifying processes and controls. *Marine Chemistry*, *157*, 144-161.

Dettman, D.L., Kohn, M.J., Quade, J., Ryerson, F.J., Ojha, T.P. and Hamidullah, S. (2001). Seasonal stable isotope evidence for a strong Asian monsoon throughout the past 10.7 my. *Geology*, *29*(1), pp.31-34.

Elliot, A.J., Cross, K.W. and Fleming, D.M. (2009). Seasonality and trends in the incidence and prevalence of gout in England and Wales 1994–2007. *Annals of the rheumatic diseases*, *68*(11), 1728-1733.

El-Shazly, S. H. (2011). Stable isotope of some selected Egyptian pectinids and their paleoenvironmental implications. *Journal of African Earth Sciences*, *59*(2-3), 283-294.

Ganguly, D., Suryanarayana, K., & Raman, M. (2021). Cyclone Ockhi induced upwelling and associated changes in biological productivity in Arabian Sea. *Marine Geodesy*, *44*(1), 70-89.

Geary, D.H., Brieske, T.A. and Bemis, B.E. (1992). The influence and interaction of temperature, salinity, and upwelling on the stable isotopic profiles of strombid gastropod shells. *Palaios*, 77-85.

Ghosh, P., Patecki, M., Rothe, M. and Brand, W.A. (2005). Calcite-CO2 mixed into CO2-free air: a new CO2-in-air stable isotope reference material for the VPDB scale. *Rapid Communications in Mass Spectrometry: An International Journal Devoted to the Rapid Dissemination of Up-to-the-Minute Research in Mass Spectrometry*, *19*(8), 1097-1119.

Ghosh, P., Prasanna, K., Banerjee, Y., Williams, I.S., Gagan, M.K., Chaudhuri, A. and Suwas, S. (2018). Rainfall seasonality on the Indian subcontinent during the Cretaceous greenhouse. *Scientific Reports*, *8*(1), 1-9.

Ghosh, P., Ramdas, L., Banerjee, Y., Thamizharasan, S. and Banerjee, S. (2021). Seasonal freshwater flux estimation using mollusc from the tropical Mandovi Zuari estuary, Goa, India. *Journal of Earth System Science*, *130*(2), p.107.

Guo, Z.T., Sun, B., Zhang, Z.S., Peng, S.Z., Xiao, G.Q., Ge, J.Y., Hao, Q.Z., Qiao, Y.S., Liang, M.Y., Liu, J.F. and Yin, Q.Z. (2008). A major reorganization of Asian climate by the early Miocene. *Climate of the Past*, *4*(3), 153-174.

Gupta, A.K., Yuvaraja, A., Prakasam, M., Clemens, S.C. and Velu, A. (2015). Evolution of the South Asian monsoon wind system since the late Middle Miocene. *Palaeogeography, Palaeoclimatology, Palaeoecology*, *438*, 160-167.

Halder, K. and Bano, S. (2015). Cenozoic Corbulidae (Bivalvia, Mollusca) from the Indian subcontinent—palaeobiogeography and revision of three species from Kutch, India. *Arabian Journal of Geosciences*, *8*, pp.2019-2034.

Harzhauser, M., Piller, W.E., Müllegger, S., Grunert, P. and Micheels, A. (2011). Changing seasonality patterns in Central Europe from Miocene Climate Optimum to Miocene Climate Transition deduced from the Crassostrea isotope archive. *Global and Planetary Change*, *76*(1-2), 77-84.

Jacob, J., Ghosh, P., Dineshbabu, A. P., Sabu, P., Srinivas, K., & Sulochanan, B. (2014). Hydrographical characteristics and oxygen isotopic signatures of water in a coastal environment (Mangalore) along the southeastern Arabian Sea. *Journal of oceanography*, *70*, 251-266.

Jones, D. S., & Allmon, W. D. (1995). Records of upwelling, seasonality and growth in stable-isotope profiles of Pliocene mollusk shells from Florida. *Lethaia*, *28*(1), 61-74.

Joshi, A.P., Chowdhury, R.R., Warrior, H.V. and Kumar, V. (2021). Influence of the freshwater plume dynamics and the barrier layer thickness on the CO2 source and sink characteristics of the Bay of Bengal. *Marine Chemistry*, *236*, 104030.

Killingley, J.S. and Berger, W.H. (1979). Stable isotopes in a mollusk shell: detection of upwelling events. *Science*, *205*(4402), 186-188.

Krantz, D. E., Kronick, A. T., & Williams, D. F. (1988). A model for interpreting continental-shelf hydrographic processes from the stable isotope and cadmium: calcium profiles of scallop shells. *Palaeogeography, Palaeoclimatology, Palaeoecology*, *64*(3-4), 123-140.

Kroopnick, P. (1980). The distribution of13C in the Atlantic Ocean. *Earth and Planetary Science Letters*, *49*(2), 469-484.

Kubota, K., Yokoyama, Y., Kawakubo, Y., Seki, A., Sakai, S., Ajithprasad, P., Maemoku, H. and Osada, T. (2015). Migration history of an ariid Indian catfish reconstructed by otolith Sr/Ca and δ18O micro-analysis. *Geochemical Journal*, *49*(5), 469-480.

Kumar, A. and Saraswati, P.K. (1997). Response of larger foraminifera to mixed carbonate-siliciclastic environments: an example from the Oligocene-Miocene sequence of Kutch, India. *Palaeogeography, Palaeoclimatology, Palaeoecology*, *136*(1-4), 53-65.

Lécuyer, C., Reynard, B. and Martineau, F. (2004). Stable isotope fractionation between mollusc shells and marine waters from Martinique Island. *Chemical Geology*, *213*(4), 293-305.

Levy, R., Harwood, D., Florindo, F., Sangiorgi, F., Tripati, R., Von Eynatten, H., Gasson, E., Kuhn, G., Tripati, A., DeConto, R. and Fielding, C. (2016). Antarctic ice sheet sensitivity to atmospheric CO2 variations in the early to mid-Miocene. *Proceedings of the National Academy of Sciences*, *113*(13), pp.3453-3458.

McConnaughey, T. (1989). 13C and 18O isotopic disequilibrium in biological carbonates: II. In vitro simulation of kinetic isotope effects. *Geochimica et Cosmochimica Acta*, *53*(1), pp.163-171.

Qu, X., Huang, G., Hou, H., Chen, Z., & Du, Y. (2022). The opposite response of the South Asian high to increasing CO2 at different heights. *Atmospheric Science Letters*, *23*(8), e1093.

Rangarajan, R., Pathak, P., Banerjee, S. and Ghosh, P. (2021). Floating boat method for carbonate stable isotopic ratio determination in a GasBench II peripheral. *Rapid Communications in Mass Spectrometry*, *35*(15), e9115.

Rao, A.D., Joshi, M. and Ravichandran, M. (2009). Observed low-salinity plume off Gulf of Khambhat, India, during post-monsoon period. *Geophysical research letters*, *36*(3).

Rao, M.R. and Verma, P. (2014). Palynological investigation of Neogene (Early Miocene) sediments of Mangalore basin, India: Palaeoenvironmental and palaeoclimatic implications. *Journal of the Geological Society of India*, *84*, 55-67.

Raymo, M.E. and Ruddiman, W.F. (1992). Tectonic forcing of late Cenozoic climate. *Nature*, *359*(6391), 117-122.

Roy Chowdhury, R., Prasanna Kumar, S., Narvekar, J., & Chakraborty, A. (2020). Back-to-back occurrence of tropical cyclones in the Arabian sea during October–November 2015: causes and responses. *Journal of Geophysical Research: Oceans*, *125*(6), e2019JC015836.

Sarr, A.C., Donnadieu, Y., Bolton, C.T., Ladant, J.B., Licht, A., Fluteau, F., Laugié, M., Tardif, D. and Dupont-Nivet, G. (2022). Neogene South Asian monsoon rainfall and wind histories diverged due to topographic effects. *Nature Geoscience*, *15*(4), pp.314-319.

Scheiner, F., Holcová, K., Milovský, R. and Kuhnert, H. (2018). Temperature and isotopic composition of seawater in the epicontinental sea (Central Paratethys) during the Middle Miocene Climate Transition based on Mg/Ca, δ18O and δ13C from foraminiferal tests. *Palaeogeography, palaeoclimatology, palaeoecology*, *495*, 60-71.

Scholz, S.R., Petersen, S.V., Escobar, J., Jaramillo, C., Hendy, A.J., Allmon, W.D., Curtis, J.H., Anderson, B.M., Hoyos, N., Restrepo, J.C. and Perez, N. (2020). Isotope sclerochronology indicates enhanced seasonal precipitation in northern South America (Colombia) during the Mid-Miocene Climatic Optimum. *Geology*, *48*(7), 668-672.

Shukla, A., Guleria, J.S. and Mehrotra, R.C. (2012). A fruit wing of Shorea Roxb. from the Early Miocene sediments of Kachchh, Gujarat and its bearing on palaeoclimatic interpretation. *Journal of Earth System Science*, *121*, 195-201.

Steinthorsdottir, M., Coxall, H.K., De Boer, A.M., Huber, M., Barbolini, N., Bradshaw, C.D., Burls, N.J., Feakins, S.J., Gasson, E., Henderiks, J. and Holbourn, A.E. (2021). The Miocene: the future of the past. *Paleoceanography and Paleoclimatology*, *36*(4), p.e2020PA004037.

Stewart, D.R., Pearson, P.N., Ditchfield, P.W. and Singano, J.M. (2004). Miocene tropical Indian Ocean temperatures: evidence from three exceptionally preserved foraminiferal assemblages from Tanzania. *Journal of African Earth Sciences*, *40*(3-4), 173-189.

Tao, K., Robbins, J.A., Grossman, E.L. and O'Dea, A. (2013). Quantifying upwelling and freshening in nearshore tropical American environments using stable isotopes in modern gastropods. *Bulletin of Marine Science*, *89*(4), 815-835.

United Nations Environment Programme (2019). GEMStat database of the Global Environment Monitoring System for freshwater (GEMS/Water) Programme. International

Centre for Water Resources and Global Change, Koblenz. Available upon request from GEMS/Water Data Centre: gemstat.org

Verma, P., Mandal, N., Thakkar, M.G., Rao, M.R. and Bajpai, S. (2013). Palynological record from Chhasra Formation (Early Miocene), Eastern Kutch, Gujarat. *Journal of Palaeosciences*, *62*(1-2)), 149-155.
Verma, P., Mandal, N., Thakkar, M.G., Rao, M.R. and Bajpai, S. (2013). Palynological record from Chhasra Formation (Early Miocene), Eastern Kutch, Gujarat. *Journal of Palaeosciences*, *62*(1-2)), 149-155.
Waite, R. and Allmon, W.D. (2013). Observations on the biology and sclerochronology of Turritella leucostoma (Valenciennes, 1832; Cerithioidea: Turritellidae) from the Gulf of California. *American Malacological Bulletin*, *31*(2), 297-310.

Watanabe, T. and Oba, T. (1999). Daily reconstruction of water temperature from oxygen isotopic ratios of a modern Tridacna shell using a freezing microtome sampling technique. *Journal of Geophysical Research: Oceans*, *104*(C9), 20667-20674.

Wei, G., Li, X.H., Liu, Y., Shao, L. and Liang, X. (2006). Geochemical record of chemical weathering and monsoon climate change since the early Miocene in the South China Sea. *Paleoceanography*, *21*(4).

Wierzbowski, H. (2007). Effects of pre-treatments and organic matter on oxygen and carbon isotope analyses of skeletal and inorganic calcium carbonate. *International Journal of Mass Spectrometry*, *268*(1), 16-29.

Yang, Y., Han, W., Ye, C., Galy, A. and Fang, X. (2022). Trends and Transitions in Silicate Weathering in the Asian Interior (NE Tibet) Since 53 Ma. *Frontiers in Earth Science*, *10*, 824404.

Zammit, R., Lear, C. H., Samankassou, E., Lourens, L. J., Micallef, A., Pearson, P. N., & Bialik, O. M. (2022). Early Miocene intensification of the North African hydrological cycle: multi-proxy evidence from the shelf carbonates of Malta. *Paleoceanography and Paleoclimatology*, *37*(9), e2022PA004414.

Zammit, R., Lear, C.H., Samankassou, E., Lourens, L.J., Micallef, A., Pearson, P.N. and Bialik, O.M. (2022). Early Miocene intensification of the North African hydrological cycle: multi-proxy evidence from the shelf carbonates of Malta. *Paleoceanography and Paleoclimatology*, *37*(9), e2022PA004414.

Zhang, R., Zhang, Z. and Jiang, D. (2018). Global Cooling Contributed to the Establishment of a Modern-Like East Asian Monsoon Climate by the Early Miocene. *Geophysical Research Letters*, *45*(21), 11-941.

Zhang, S., Qu, X., Huang, G., & Hu, P. (2023). Asymmetric response of South Asian summer monsoon rainfall in a carbon dioxide removal scenario. *npj Climate and Atmospheric Science*, *6*(1), 10.

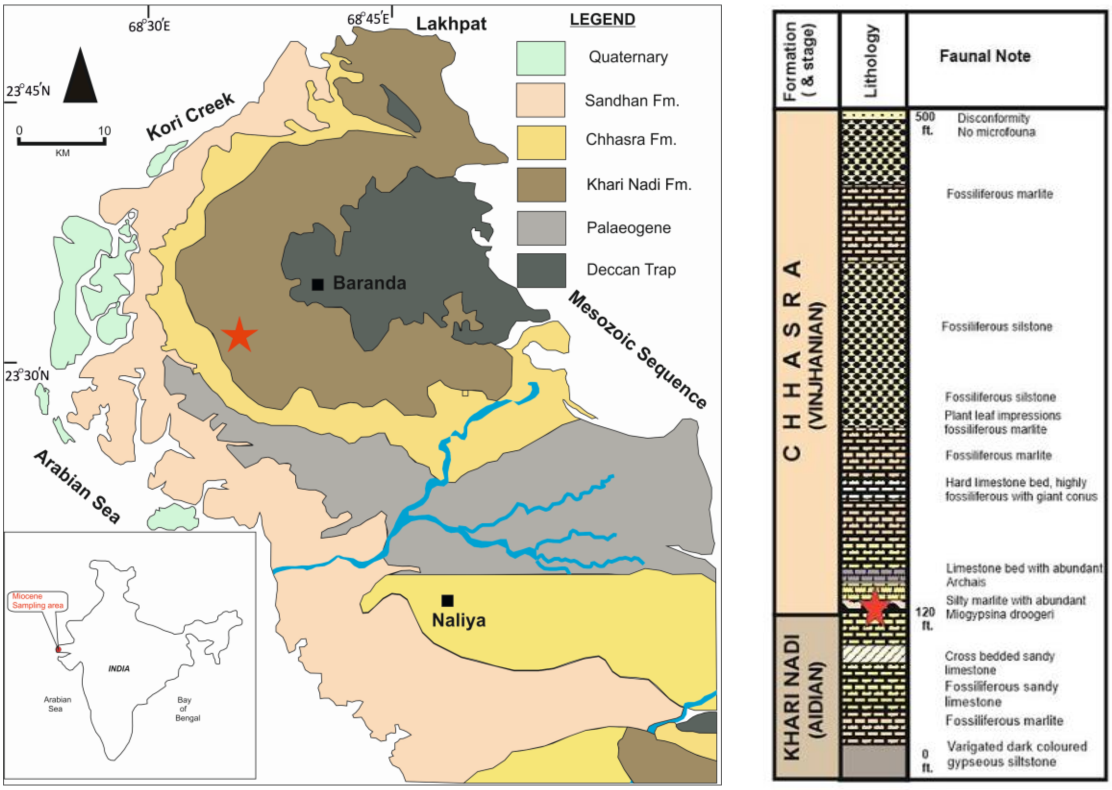

Figure 1: Geological map of the Kachchh Basin and Cenozoic lithologies (modified after (Biswas, 1992)). The sampling location of the present study is indicated by a red asterisk. Laterally, in the display, we provided lithostratigraphic information summarizing the sedimentation in the Kachchh Basin during the early-mid Miocene time period. We showed here the litho-units of Khari Nadi and Chhasra Formations and their faunal assemblages (Biswas, 1992; Kumar & Saraswati, 1997). The red asterisk indicates the position of the *Turritella* bed.

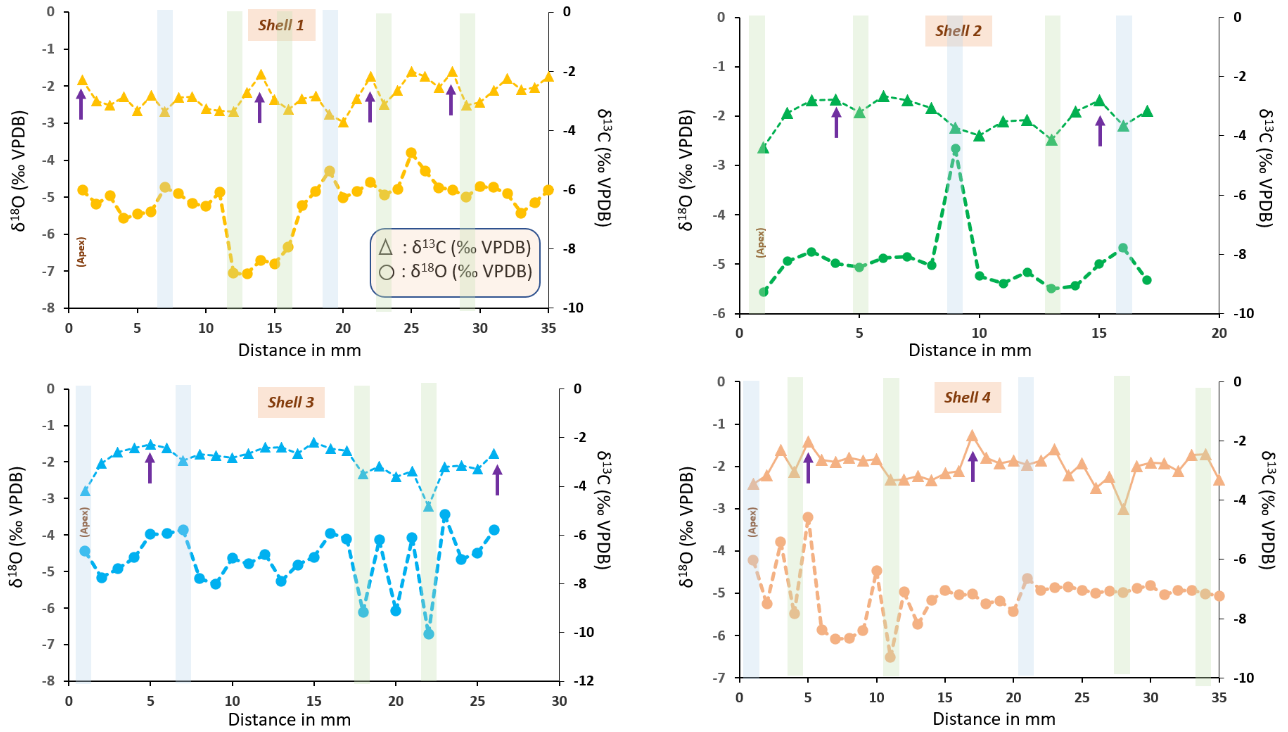

Figure 2: Stable carbon (triangle) and oxygen (circle) isotope profiles for the early Miocene *Turritella sp.* from the Kachchh basin investigated in this study. The purple arrows in the $\delta^{13}C$ profile indicates periods of highest productivity. The green bars with the depletion in both $\delta^{13}C$ and $\delta^{18}O$ represent the episodes of freshwater run-off; the blue bars with depletion in $\delta^{13}C$ and enrichment in $\delta^{18}O$ represent episodes of upwelling.

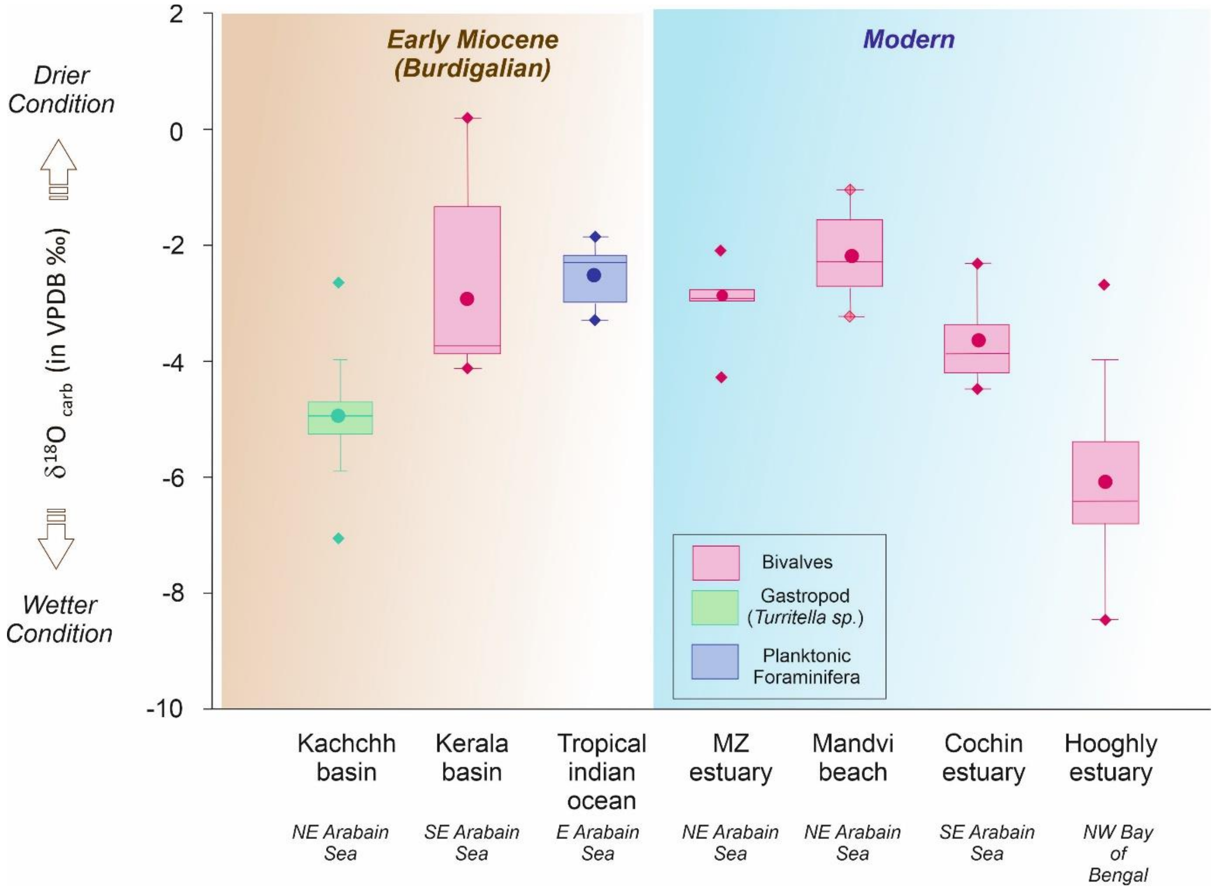

Figure 3: Comparison of $\delta^{18}O_{carb}$ record of the Kachchh basin from the present study with the other coeval records from Quilon formation, Kerala basin (Prasanna and Kapur 2022), tropical coastal Indian ocean (Stewart et al., 2004) and modern Indian coastal-estuarine environments. For the modern $\delta^{18}O$ records, we have taken data from Ghosh et al., 2021 (MZ estuary), Ghosh et al., 2018 (Cochin estuary) and Banerjee et al., 2018 (Hooghly estuary). Rationale for comparison of different $\delta^{18}O_{carb}$ record across genera is given in the supplementary document S6.

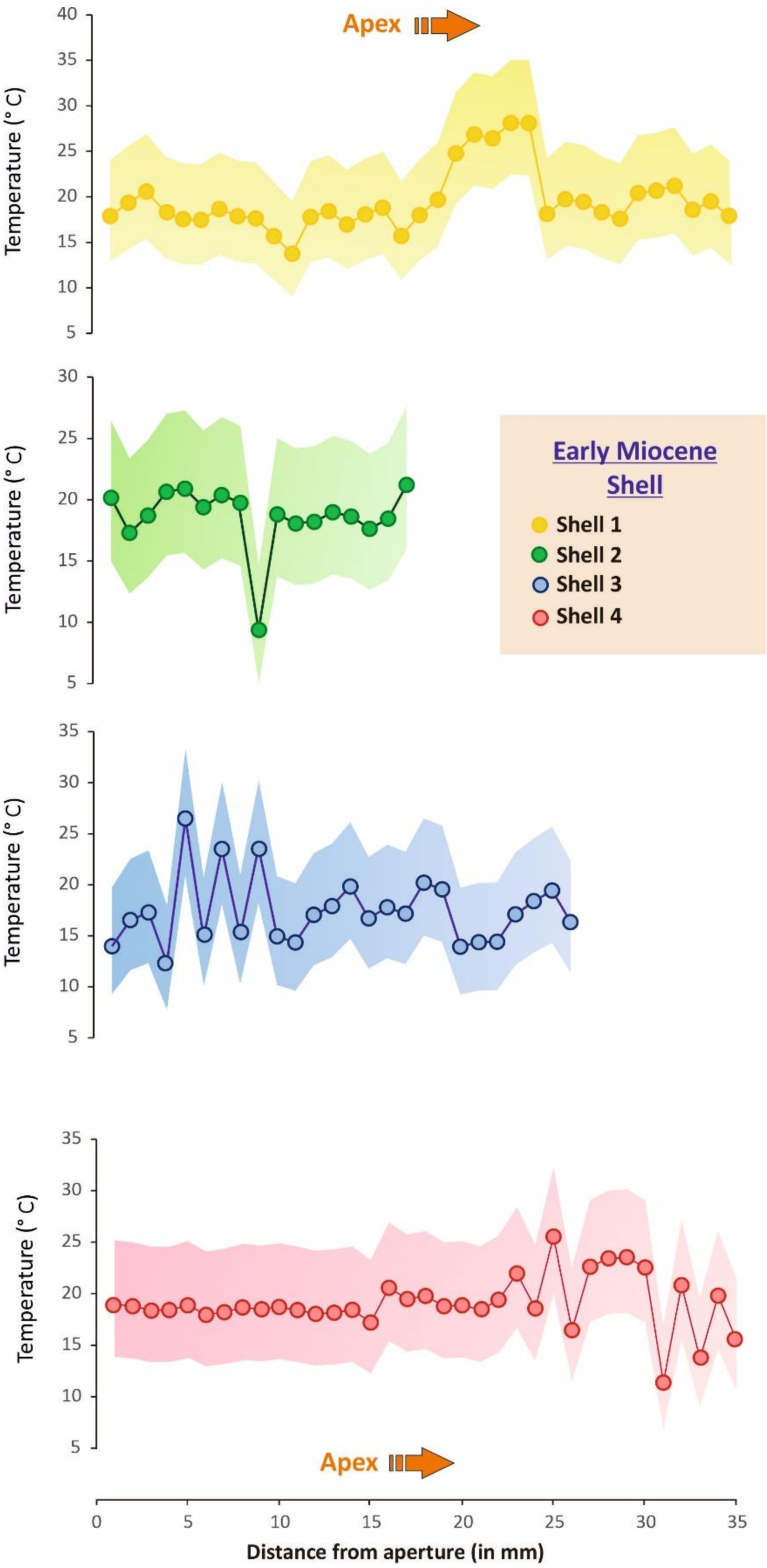

Figure 4 A: Temperature estimates for the early Miocene northeastern Arabian sea retrieved from the *Turritella* sp. growth bands based on conventional oxygen isotope thermometry. We have used Arthur and Anderson 1982 equation to retrieve the temperature from the $\delta^{18}O_{shell}$. Uncertainties (shaded region) were calculated based on different $\delta^{18}O_{water}$ compositions (see text for the explanations).

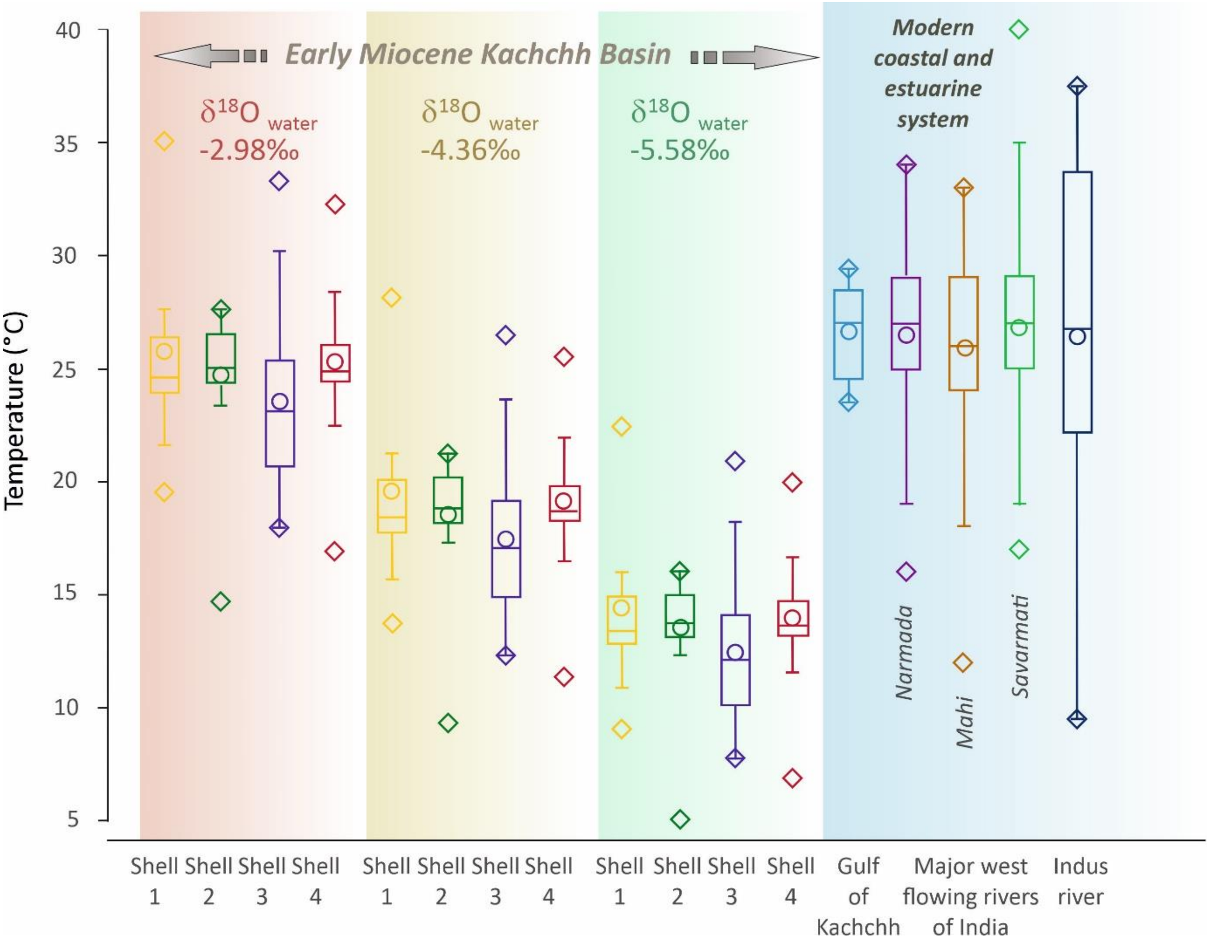

Figure 4 B: The estimated early Miocene temperatures (with different assumed $\delta^{18}O_{water}$ composition) were compared with the modern NE Arabian sea temperature at the Gulf of Kachchh (Nandkeolyar et al., 2013) and temperature variabilities of major west flowing river estuaries of India (GEMStat data repository http://gemstat.org/) and Indus river estuarine system (Kalhoro et al 2017).

Table 1: Summary of the temperature estimated from *Turritella* shell carbonate $\delta^{18}O$ compositions assuming different $\delta^{18}O_{water}$ compositions (‰ VSMOW scale). We have used the oxygen isotope thermometry equation given by Arnold and Arthur 1983 for estimating the temperature.

Shell number	**$\delta^{18}O_{water}$ =-4.36‰**	**$\delta^{18}O_{water}$ = -5.58‰**	**$\delta^{18}O_{water}$ = -2.98‰**	**$\delta^{18}O_{water}$ = -0.4‰**
Shell 1	T_{min} = 13.75°C T_{max} = 28.13°C	T_{min} = 9.07°C T_{max} = 22.41°C	T_{min} = 19.51°C T_{max} = 35.06°C	T_{min} = 31.58°C T_{max} = 49.27°C
Shell 2	T_{min} = 9.34°C T_{max} = 21.21°C	T_{min} = 5.02°C T_{max} = 15.96°C	T_{min} = 14.69°C T_{max} = 27.60°C	T_{min} = 26.00°C T_{max} = 40.83°C
Shell 3	T_{min} = 12.31°C T_{max} = 26.48°C	T_{min} = 7.74°C T_{max} = 20.87°C	T_{min} = 17.94°C T_{max} = 33.28°C	T_{min} =29.77°C T_{max} = 47.28°C
Shell 4	T_{min} = 11.36°C T_{max} = 25.51°C	T_{min} = 6.87°C T_{max} = 19.97°C	T_{min} = 16.90°C T_{max} = 32.24°C	T_{min} = 28.57°C T_{max} = 46.10°C

Supplementary Material

S1:

Table 1: Stable isotope data of the early Miocene gastropod shells investigated in this study:

Shell	Distance from Apex (in mm)	δ^{13}C (‰ VPDB)	δ^{18}O (‰ VPDB)
Shell 1	1	-2.28	-4.81
	2	-2.99	-5.18
	3	-3.15	-4.97
	4	-2.86	-5.57
	5	-3.34	-5.46
	6	-2.81	-5.39
	7	-3.35	-4.73
	8	-2.89	-4.91
	9	-2.86	-5.17
	10	-3.27	-5.24
	11	-3.33	-4.87
	12	-3.36	-7.05
	13	-2.71	-7.06
	14	-2.11	-6.71
	15	-2.95	-6.80
	16	-3.29	-6.35
	17	-2.94	-5.23
	18	-2.84	-4.84
	19	-3.45	-4.29
	20	-3.72	-5.01
	21	-2.94	-4.85
	22	-2.18	-4.59
	23	-3.13	-4.94
	24	-2.64	-4.78
	25	-2.01	-3.81
	26	-2.18	-4.28
	27	-2.55	-4.75
	28	-2.01	-4.80
	29	-3.14	-4.99
	30	-3.04	-4.71
	31	-2.64	-4.73
	32	-2.24	-4.91
	33	-2.62	-5.43
	34	-2.55	-5.15
	35	-2.17	-4.81
Shell 2	1	-4.39	-5.57
	2	-3.22	-4.94

	3	-2.81	-4.75
	4	-2.77	-4.98
	5	-3.20	-5.06
	6	-2.66	-4.88
	7	-2.80	-4.85
	8	-3.07	-5.02
	9	-3.72	-2.66
	10	-3.98	-5.24
	11	-3.51	-5.39
	12	-3.47	-5.16
	13	-4.13	-5.50
	14	-3.18	-5.44
	15	-2.80	-5.00
	16	-3.65	-4.67
	17	-3.16	-5.33
Shell 3	1	-4.19	-4.44
	2	-3.07	-5.17
	3	-2.59	-4.92
	4	-2.42	-4.62
	5	-2.27	-3.97
	6	-2.41	-3.96
	7	-2.95	-3.85
	8	-2.67	-5.19
	9	-2.74	-5.34
	10	-2.82	-4.64
	11	-2.64	-4.79
	12	-2.41	-4.53
	13	-2.40	-5.26
	14	-2.66	-4.81
	15	-2.20	-4.61
	16	-2.46	-3.95
	17	-2.54	-4.10
	18	-3.48	-6.11
	19	-3.18	-4.13
	20	-3.60	-6.08
	21	-3.37	-4.08
	22	-4.83	-6.72
	23	-3.21	-3.44
	24	-3.14	-4.67
	25	-3.28	-4.49
	26	-2.66	-3.86
Shell 4	1	-3.45	-4.22
	2	-3.16	-5.25
	3	-2.31	-3.79
	4	-3.04	-5.49
	5	-2.02	-3.20

	6	-2.63	-5.87
	7	-2.71	-6.09
	8	-2.57	-6.06
	9	-2.66	-5.88
	10	-2.61	-4.47
	11	-3.30	-6.51
	12	-3.30	-4.97
	13	-3.18	-5.74
	14	-3.33	-5.16
	15	-3.08	-4.93
	16	-3.02	-5.04
	17	-1.80	-5.02
	18	-2.56	-5.24
	19	-2.75	-5.17
	20	-2.67	-5.42
	21	-2.81	-4.65
	22	-2.66	-4.93
	23	-2.28	-4.87
	24	-3.15	-4.84
	25	-2.75	-4.93
	26	-3.59	-5.00
	27	-3.21	-4.95
	28	-4.30	-4.98
	29	-2.85	-4.88
	30	-2.74	-4.82
	31	-2.77	-5.04
	32	-3.01	-4.93
	33	-2.46	-4.92
	34	-2.44	-5.01
	35	-3.31	-5.06

S2: Mode of preservation of the samples:

Fig S2: In the field, we documented three different modes of preservation for the *Turritella* samples in three different strata: Type (A) well-preserved samples with white shining lustre; Type (B) poorly preserved samples with greenish-yellow dull lustre; Type (C) Poorly preserved with a reddish yellow dull lustre. Only Type (A) samples with well preservation were screened for the isotopic investigation.

S3: XRD spectra of the shell:

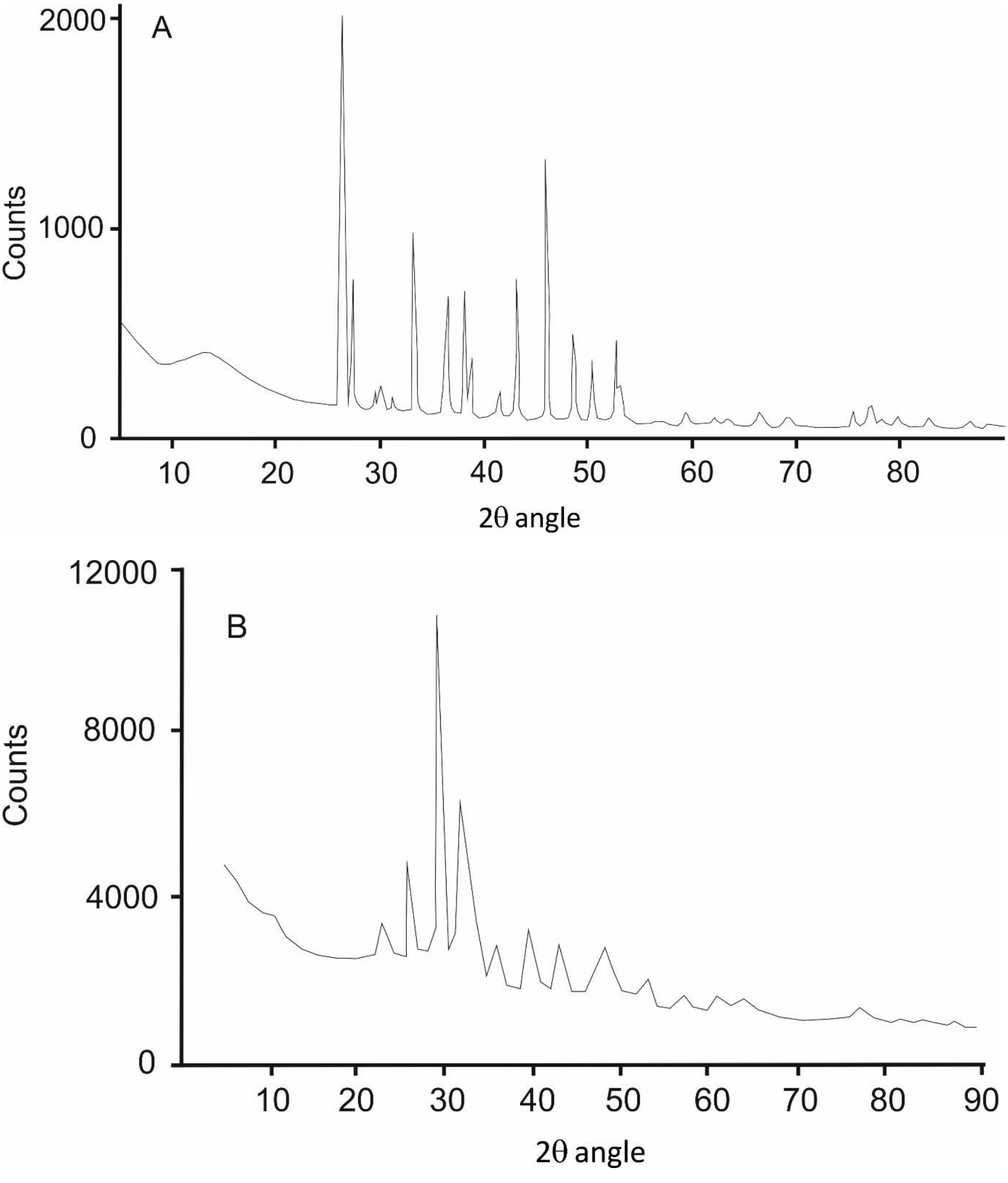

Fig S3: (A) XRD spectra of the aragonite sample investigated in this study for the isotopic investigations. (B) XRD spectra of the samples showing aragonite mineralogy mixed with calcite. These were not considered for the isotopic investigations.

<u>S4: Sampling protocol</u>

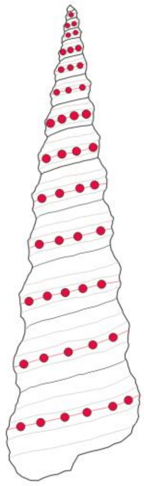

Fig S4: Schematic representation of the sampling method along the center of each whorl following the growth axis of the *Turritella sp.* shell. The same protocol was followed for each of the samples investigated in this study.

<u>S5. A: Correlation between δ^{13}C-δ^{18}O for the shells:</u>

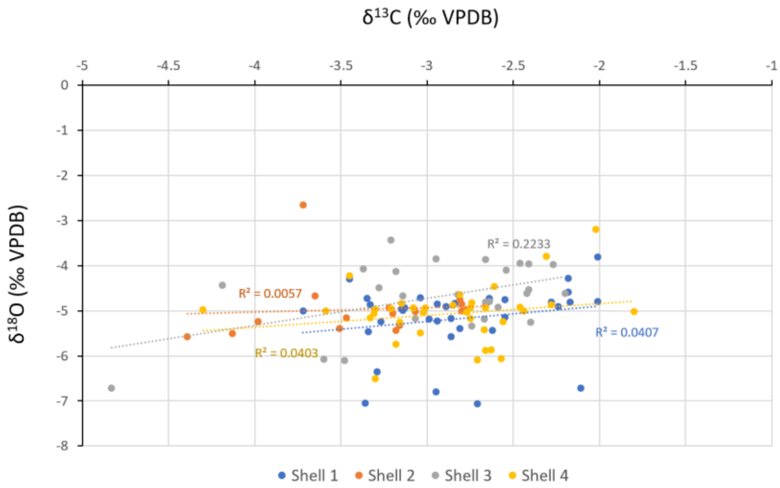

Shell	R^2	*p*-Value
Shell 1	0.040	1.69E-18
Shell 2	0.005	2.60E-07
Shell 3	0.22	4.38E-12
Shell 4	0.040	2.06E-19

Fig S5.A: Correlation between δ^{13}C and δ^{18}O for all the *Turritella* shells investigated in this study.

S5. B: $\delta^{13}C$ variability

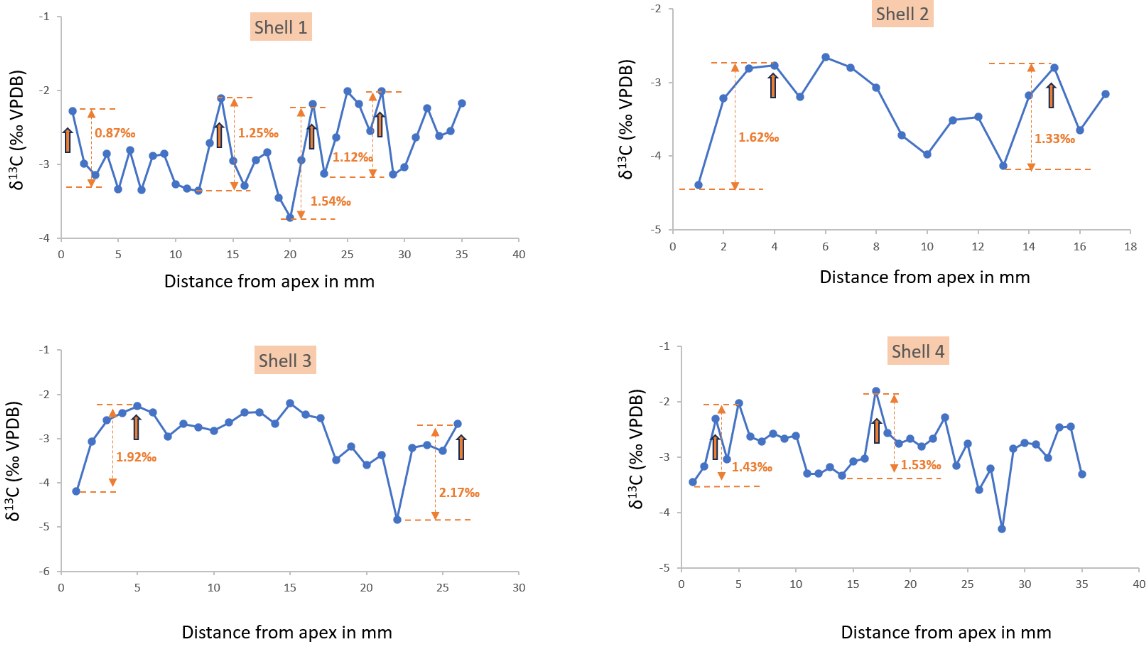

Fig S5. B: Figure showing periodic variability in the $\delta^{13}C$max values (bold arrows) and amplitude of $\delta^{13}C$ change from the nearest base level.

S6 :Comparison of early Miocene *Turritella* $\delta^{18}O$ record from Kachchh basin with other co-eval as well as modern records:

S6. A: Sample locations:

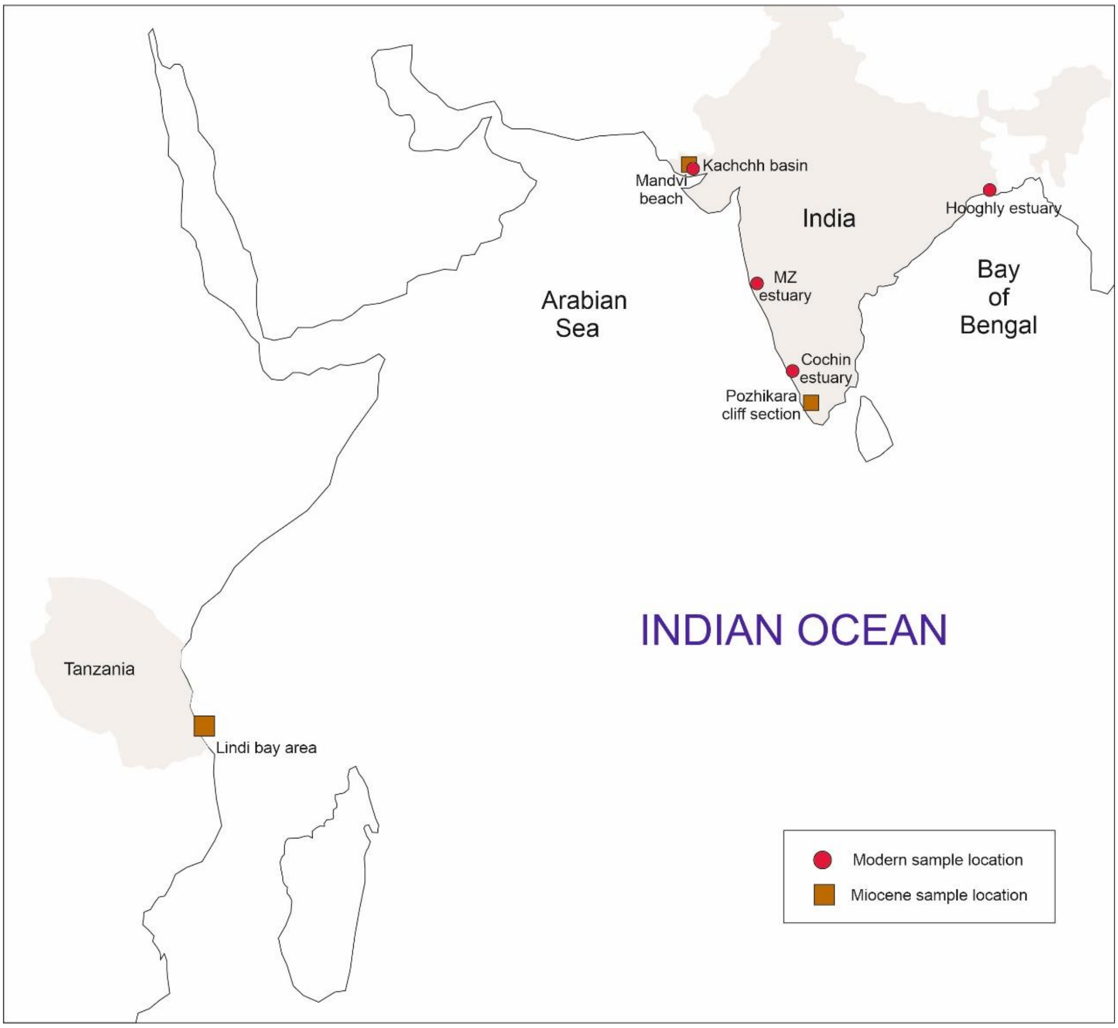

Map showing the sample locations from the part of the Indo-African sector of the Indian ocean, as discussed in this study (Section 4.2 of the main text). Early Miocene samples investigated in this study was collected from the Kachchh basin.

S6. B: The rationale for comparing oxygen isotope records from different archives:

a) All the mollusk shells are aragonitic in nature, retaining their primary mineralogy. The foraminifera investigated by Stewart et al., 2004 are exceptionally well-preserved glassy forams. Thus, all the archives used for the comparison have shown no effect of alteration.

b) The stable isotope data used for the comparison are from already published literature that documented negligible kinetic effects in respective cases.

c) All the organisms grew in equilibrium with the ambient water condition of the coastal shelf region. Thus, their shell carbonate stable isotope profile would capture changes in the hydrological conditions of the shelf region.

d) Previous investigations have also shown that the oxygen isotope records from different mollusc species living in the same environment could be used for reconstructing hydrological conditions (Le´cuyer et al., 2004; Latal et al., 2006; Toth et al., 2010; Clauzel et al., 2020).

e) A study by Bice et al., 2003 has shown the stable isotope record from glassy forams is comparable to that of the mollusc shells from nearby locations.

S7: Estimation of the change in the palaeosalinity

Assuming different $\delta^{18}O_{water}$ compositions (Section 4.3 of the main text), we obtained an overall temperature range varying from a minimum 5.02°C to a maximum of 35.06°C with an average 19.13°C. We have calculated salinity (S) at three different temperatures T_{min} 5.02°C, T_{max} 35.06°C and $T_{average}$ 19.13°C. First, we calculated the fractionation factor at each of these temperatures and then calculated $\delta^{18}O_{water}$ from $\delta^{18}O_{carbonate}$. Three different $\delta^{18}O_{water}$ -S relationships were used in order to calculate the salinity from the calculated $\delta^{18}O_{water}$. These equations are: $\delta^{18}O_{water}$ -S relationships at the Northern Indian Ocean given by Kumar et al., 2018; summer and winter time relationship at the coastal Arabian sea given by Deshpande et al., 2013. We have taken an average of the salinities calculated using each of these equations and derived ΔS (S_{max}-S_{min}) in order to estimate the change in the salinity due to freshwater influx. The ΔS is around 21 psu for the NE coastal Arabian sea (west coast of India) during early Miocene. Model based study suggested change in the salinity of comparable magnitude for the modern SW coastal India driven by freshwater discharge (Seena et al., 2019).

<u>References</u>

Bice, K. L., Huber, B. T., & Norris, R. D. (2003). Extreme polar warmth during the Cretaceous greenhouse? Paradox of the late Turonian δ18O record at Deep Sea Drilling Project Site 511. *Paleoceanography*, *18*(2).

Clauzel, T., Maréchal, C., Fourel, F., Barral, A., Amiot, R., Betancort, J.F., Lomoschitz, A., Meco, J. and Lécuyer, C. (2020). Reconstruction of sea-surface temperatures in the Canary Islands during Marine Isotope Stage 11. *Quaternary Research*, *94*, pp.195-209.

Deshpande, R.D., Muraleedharan, P.M., Singh, R.L., Kumar, B., Rao, M.S., Dave, M., Sivakumar, K.U. and Gupta, S.K. (2013). Spatio-temporal distributions of δ18O, δD and salinity in the Arabian Sea: identifying processes and controls. *Marine Chemistry*, *157*, pp.144-161.

Kumar, P. K., Singh, A., & Ramesh, R. (2018). Controls on δ18O, δD and δ18O-salinity relationship in the northern Indian Ocean. *Marine Chemistry*, *207*, 55-62.

Latal, C., Piller, W. E., & Harzhauser, M. (2006). Shifts in oxygen and carbon isotope signals in marine molluscs from the Central Paratethys (Europe) around the Lower/Middle Miocene transition. *Palaeogeography, Palaeoclimatology, Palaeoecology*, *231*(3-4), 347-360.

Lécuyer, C., Reynard, B., & Martineau, F. (2004). Stable isotope fractionation between mollusc shells and marine waters from Martinique Island. *Chemical Geology*, *213*(4), 293-305.

Seena, G., Muraleedharan, K. R., Revichandran, C., Abdul Azeez, S., & John, S. (2019). Seasonal spreading and transport of buoyant plumes in the shelf off Kochi, South west coast of India-A modeling approach. *Scientific Reports*, *9*(1), 19956.

Stewart, D. R., Pearson, P. N., Ditchfield, P. W., & Singano, J. M. (2004). Miocene tropical Indian Ocean temperatures: evidence from three exceptionally preserved foraminiferal assemblages from Tanzania. *Journal of African Earth Sciences*, *40*(3-4), 173-189.

Tóth, E., Görög, Á., Lécuyer, C., Moissette, P., Balter, V., & Monostori, M. (2010). Palaeoenvironmental reconstruction of the Sarmatian (Middle Miocene) Central Paratethys based on palaeontological and geochemical analyses of foraminifera, ostracods, gastropods and rodents. *Geological Magazine*, *147*(2), 299-314.